Sfrp4 repression of the Ror2/Jnk cascade in osteoclasts protects cortical bone from excessive endosteal resorption

Kun Chen[a,1], Pei Ying Ng[a], Ruiying Chen[a], Dorothy Hu[a], Shawn Berry[a], Roland Baron[a,b,c], and Francesca Gori[a,2]

[a]Division of Bone and Mineral Research, Department of Oral Medicine, Infection, and Immunity, Harvard School of Dental Medicine, Boston, MA 02115; [b]Department of Medicine, Harvard Medical School, Boston, MA 02115; and [c]Endocrine Unit, Massachusetts General Hospital, Boston, MA 02114

Edited by Karl L. Insogna, Yale University School of Medicine, and accepted by Editorial Board Member Lia Addadi June 5, 2019 (received for review January 17, 2019)

Loss-of-function mutations in the Wnt inhibitor secreted frizzled receptor protein 4 (SFRP4) cause Pyle's disease (OMIM 265900), a rare skeletal disorder characterized by wide metaphyses, significant thinning of cortical bone, and fragility fractures. In mice, we have shown that the cortical thinning seen in the absence of *Sfrp4* is associated with decreased periosteal and endosteal bone formation and increased endocortical resorption. While the increase in Rankl/Opg in cortical bone of mice lacking *Sfrp4* suggests an osteoblast-dependent effect on endocortical osteoclast (OC) activity, whether Sfrp4 can cell-autonomously affect OCs is not known. We found that *Sfrp4* is expressed during bone marrow macrophage OC differentiation and that Sfrp4 significantly suppresses the ability of early and late OC precursors to respond to Rankl-induced OC differentiation. *Sfrp4* deletion in OCs resulted in activation of canonical Wnt/β-catenin and noncanonical Wnt/Ror2/Jnk signaling cascades. However, while inhibition of canonical Wnt/β-catenin signaling did not alter the effect of *Sfrp4* on OCgenesis, blocking the noncanonical Wnt/Ror2/Jnk cascade markedly suppressed its regulation of OC differentiation in vitro. Importantly, we report that deletion of *Ror2* exclusively in OCs (*CtskCreRor2*$^{fl/fl}$) in *Sfrp4* null mice significantly reversed the increased number of endosteal OCs seen in these mice and reduced their cortical thinning. Altogether, these data show autocrine and paracrine effects of Sfrp4 in regulating OCgenesis and demonstrate that the increase in endosteal OCs seen in *Sfrp4*$^{-/-}$ mice is a consequence of noncanonical Wnt/Ror2/Jnk signaling activation in OCs overriding the negative effect that activation of canonical Wnt/β-catenin signaling has on OCgenesis.

Sfrp4 | Ror2/Jnk | endocortical remodeling | Pyle's disease | Wnt signaling

Cortical bone fragility is a major contributor to osteoporotic nonvertebral fractures and regulation of osteoclastogenesis is central for understanding diseases associated with low bone mass. Despite the importance of cortical bone, little is known about the specific regulation of cortical bone thickness and density. Activation of Wnt signaling, in particular the β-catenin–dependent (canonical) cascade, exerts a positive action on skeletal homeostasis, both through an increase in bone formation and an osteoprotegerin (OPG)-dependent decrease in bone resorption (1). The Wnt pathway comprises several soluble inhibitors that could potentially be appropriate targets or biologics for therapeutic intervention (1, 2). Among these inhibitors is the family of secreted frizzled receptors (Sfrp1 to 5), which bind directly to Wnts interfering with their ability to interact with the receptor complexes (1, 3). Thus, different from sclerostin and Dkk1, which block canonical Wnt/β-catenin signaling (1), Sfrps have a more pleiotropic impact on the Wnt signaling as they can block both canonical and noncanonical Wnt cascades, and consequently might have more complex effects on tissue development and homeostasis (1, 3–5). Unlike the other Sfrps and directly relevant to osteoporosis in humans, *SFRP4* has been found associated with bone mineral density, including cortical sites, in several independent genome-wide association studies (6–9). In mice, *Sfrp4* expression is markedly increased in osteopenic accelerated-aging SAMP6 mice and manipulations of *Sfrp4*, globally or specifically in cells of the osteoblast lineage, lead to specific trabecular and cortical bone phenotypes (10–12). We have recently shown that *SFRP4* loss-of function mutations cause Pyle's disease (OMIM 265900) (13), a rare autosomal recessive skeletal dysplasia characterized, in both genders, by wide metaphyses with increased trabecular bone, significant cortical thinning, fractures, and thin calvarium (13–21). In female and male mice, *Sfrp4* genetic inactivation causes skeletal deformities closely mimicking those seen in humans: increased trabecular bone formation and decreased cortical thickness, due to impaired periosteal and endosteal bone formation and increased endosteal resorption (13). On the endosteal surface, *Sfrp4* has been reported to be expressed by bone-lining cells and osteoblasts (OBs) (10, 11, 13, 22) and the increase in Rankl/Opg in *Sfrp4* null cortical bone (13) suggests that Sfrp4 is involved in OB-dependent endosteal resorption. However, whether Sfrp4 has a cell-autonomous effect on the OC lineage is not known. A direct effect of canonical Wnt/β-catenin signaling on OCgenesis has been reported, as mice lacking β-catenin in OC precursors develop osteoporosis (23) and activation of β-catenin in vitro

Significance

Cortical bone homeostasis combines periosteal bone formation and endocortical remodeling. Flaws in these processes lead to altered cortical bone mass. Yet, little is known about the regulatory specificities of the endocortical vs. the periosteal surfaces, both critical in determining cortical thickness. We have shown that Pyle's disease is due to loss-of-function mutations in the Wnt antagonist SFRP4 and that its deletion in mice causes skeletal deformities closely mimicking those seen in Pyle's disease: cortical bone thinning. Here, we further elucidate the mechanism by which cortical bone is affected and report that both osteoblast- and osteoclast-expressed Sfrp4 regulate osteoclastogenesis and that Sfrp4-dependent suppression of the noncanonical Wnt/Ror2/Jnk cascade in osteoclasts protects cortical bone from excessive endocortical resorption.

Author contributions: K.C., R.B., and F.G. designed research; K.C., P.Y.N., R.C., S.B., and F.G. performed research; D.H. assisted with histology and sectioning of the samples; S.B. assisted with μCT scanning; K.C. and F.G. analyzed data; and K.C., R.B., and F.G. wrote the paper.

The authors declare no conflict of interest.

This article is a PNAS Direct Submission. K.L.I. is a guest editor invited by the Editorial Board.

[1]Present address: Department of Orthopedics, The First Affiliated Hospital of USTC, Division of Life Sciences and Medicine, University of Science and Technology of China, Hefei, Anhui 230001, P.R. China.

[2]To whom correspondence may be addressed. Email: francesca_gori@hsdm.harvard.edu.

This article contains supporting information online at www.pnas.org/lookup/suppl/doi:10.1073/pnas.1900881116/-/DCSupplemental.

Published online June 25, 2019.

Table 1. Bone histomorphometry analysis of cortical bone in 5-wk-old mice

	$Ror2^{fl/fl}Sfrp4^{+/+}$ (n = 5)	$Ror2_{OC}Sfrp4^{+/+}$ (n = 5)	$Ror2^{fl/fl}Sfrp4^{-/-}$ (n = 5)	$Ror2_{OC}Sfrp4^{-/-}$ (n = 4)	Interaction	Ror2	Sfrp4
Ct.Th, mm	0.1558 ± 0.005	0.1630 ± 0.001	0.082 ± 0.003^{ab}	$0.125 \pm 0.004^{a,b,c}$	$P < 0.005$	$P < 0.0005$	$P < 0.0001$
Ct.BV/TV, %	39.12 ± 1.328	40.59 ± 1.1	$20.35 \pm 1.01^{a,b}$	$30.11 \pm 1.516^{a,b,c}$	$P < 0.005$	$P < 0.0005$	$P < 0.0001$
En.N.Oc/BS, /mm	2.507 ± 0.1928	1.407 ± 0.2894	$8.469 \pm 0.90^{a,b}$	3.086 ± 0.447^{c}	$P < 0.005$	$P < 0.0001$	$P < 0.0001$
En.Oc.S/BS, %	8.105 ± 0.7838	5.212 ± 1.281	$27.74 \pm 1.69^{a,b}$	$10.19 \pm 2.13^{b,c}$	$P < 0.0005$	$P < 0.0001$	$P < 0.0001$
En.MAR, μm/d	4.039 ± 0.45	4.281 ± 0.379	$2.995 \pm 0.396^{a,b}$	$1.996 \pm 0.372^{a,b}$	NS	NS	$P < 0.001$
En.BFR, $\mu m^3 \cdot \mu m^{-2} \cdot d^{-1}$	3.153 ± 0.411	3.484 ± 0.399	$1.884 \pm 0.360^{a,b}$	$1.254 \pm 0.329^{a,b}$	NS	NS	$P < 0.0005$

Two-way ANOVA followed by Tukey's post hoc test: $a < 0.05$ compared with $Ror2^{fl/fl}Sfrp4^{+/+}$ mice, $b < 0.05$ compared with $Ror2_{OC}Sfrp4^{+/+}$ mice, $c < 0.05$ compared with $Ror2^{fl/fl}Sfrp4^{-/-}$ mice. NS, not significant; Ct.Th, cortical thickness; Ct.BV/TV, cortical bone volume/total volume; En.N.Oc/BS, endosteal osteoclast number/bone surface; En.OC.S/BS, endosteal osteoclast surface/bone surface; En.MAR, endosteal mineral apposition rate; En.BFR, endosteal bone formation rate.

inhibits OC differentiation (24, 25). In addition, Wei et al. (26) have reported that while β-catenin activation favors OC proliferation of early precursor cells, its signal must be suppressed to have mature OCs. However, to complicate matters, it has been recently reported that expression of constitutively active β-catenin in OCs in vivo leads to increased OCgenesis (27). On the other hand, several pieces of evidence indicate that noncanonical Wnt signaling activation favors OCgenesis (28–30). Here, we show that *Sfrp4* is expressed in Rankl-induced OCs and that Sfrp4 significantly suppresses their ability to respond to Rankl-induced OC differentiation. We show that Sfrp4 regulates cortical bone mass by modulating endosteal OC differentiation and function via blocking the noncanonical Wnt/Ror2/Jnk cascade in OCs. Since deregulated endosteal bone remodeling is a determinant of cortical thickness and porosity, insights gained from Sfrp4-mediated signaling in this compartment may therefore have a broad impact on our understanding of cortical biology and bone fragility.

Results

Sfrp4 Cell-Autonomously Regulates Osteoclast Differentiation and Activity. Sfrp4 is a major determinant of both cortical and trabecular bone (13) and is equally expressed in these two bone compartments (*SI Appendix*, Fig. S1*A*). In cortical bone, $Sfrp4^{-/-}$ mice display an increased number of endosteal OCs (Table 1) (13) and the increase in *Rankl*/*Opg* ratio seen in the cortical bone of these mice (13) suggests an Sfrp4 osteoblast-dependent effect on OCgenesis. As shown in Fig. 1*A*, *Sfrp4* is also expressed by bone marrow macrophages (BMMs) and its expression increases significantly during Rankl-induced OCgenesis. We found that OC formation was significantly enhanced in $Sfrp4^{-/-}$ cultures compared with wild-type (*wt*) cultures, as indicated by the increase in tartrate-resistant acid phosphatase ($TRAP^+$) multinucleated cells (MNCs) and the expression of OC-specific genes including *Nfatc1*, *c-fos*, *Rank*, *Dc-Stamp*, *Trap*, and *Cathepsin K* (*CtsK*) (Fig. 1 *B*–*D*). Moreover, in the absence of *Sfrp4*, OC activity was also significantly increased as shown by the area of resorption pits on the dentin slides seeded with $Sfrp4^{-/-}$ cultures (Fig. 1 *E* and *F*). Thus, these results indicate that OC-expressed *Sfrp4* cell-autonomously regulates OC differentiation and activity. Of note, *Sfrp1* and *Sfrp2* gene expression, but not that of *Sfrp3* and *Sfrp5*, was increased in $Sfrp4^{-/-}$ cultures compared with *wt* cultures (*SI Appendix*, Fig. S1*B*). Supporting a role for Sfrp4 in OCgenesis, we found that sFrp4 treatment dose-dependently suppresses the ability of BMMs to respond to Rankl-induced OC differentiation (Fig. 2). To confirm these paracrine and autocrine effects of Sfrp4, we performed mixed-and-matched cocultures of calvarial OBs (cOBs) and BMMs isolated from *wt* or $Sfrp4^{-/-}$ mice. We first asked whether *Sfrp4* expression is mainly expressed by cOBs or OCs and found that its expression was similar in these cell types (Fig. 3*A*). A significantly higher number of $TRAP^+$ MNCs were formed in $Sfrp4^{-/-}$ cOB/*wt* BMM cocultures and *wt* cOB/$Sfrp4^{-/-}$ BMM cocultures than in *wt* cOB/*wt* BMM cocultures. Importantly, an additive effect was found when $Sfrp4^{-/-}$ cOBs were cocultured with $Sfrp4^{-/-}$ BMMs (Fig. 3 *B* and *C*). We then treated BMMs with or without sFrp4 2 d after inducing OCgenesis and found that the number of $TRAP^+$ MNCs was significantly decreased in the sFrp4-treated cells compared with untreated cells (*SI Appendix*, Fig. S1 *C* and *D*), suggesting that Sfrp4-regulated signaling can modulate early and late OC precursor differentiation. Importantly, as shown in *SI Appendix*, Fig. S2, TUNEL assay clearly showed that Sfrp4 suppresses OCgenesis without affecting cell viability. Collectively, these findings reveal combined OC- and OB-expressed Sfrp4 effects on OCgenesis, likely reflecting the in vivo phenotype seen on the endosteal surface of $Sfrp4^{-/-}$ mice (13).

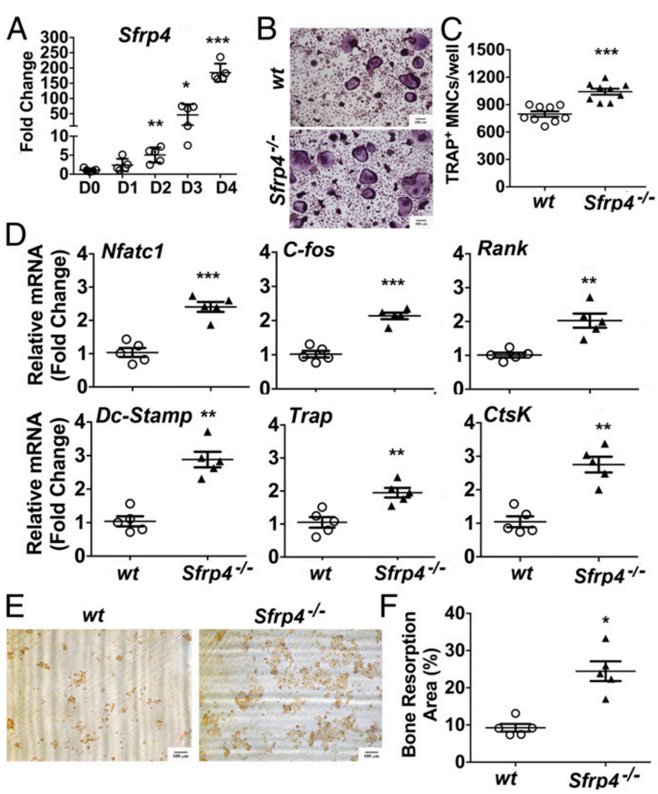

Fig. 1. Sfrp4 cell-autonomously regulates OC differentiation and activity. (*A*) *Sfrp4* expression during Rankl-induced OCgenesis of *wt* BMMs (n = 5). (*B* and *C*) TRAP staining (*B*) and quantification (*C*) in *wt* and $Sfrp4^{-/-}$ cultures (n = 9). (*D*) OC-specific gene expression in *wt* and $Sfrp4^{-/-}$ OCs (n = 5). (*E* and *F*) Pit assay: representative images of dentin seeded with *wt* or $Sfrp4^{-/-}$ cells (*E*) and quantification (*F*) of bone resorption area (n = 5). All data are mean ± SEM; open circles, *wt*; black triangles, $Sfrp4^{-/-}$ cells. $^*P < 0.05$, $^{**}P < 0.005$, $^{***}P < 0.0001$. Student's *t* test vs. day (D)0 or vs. *wt* cells. (Scale bars, 100 μm.)

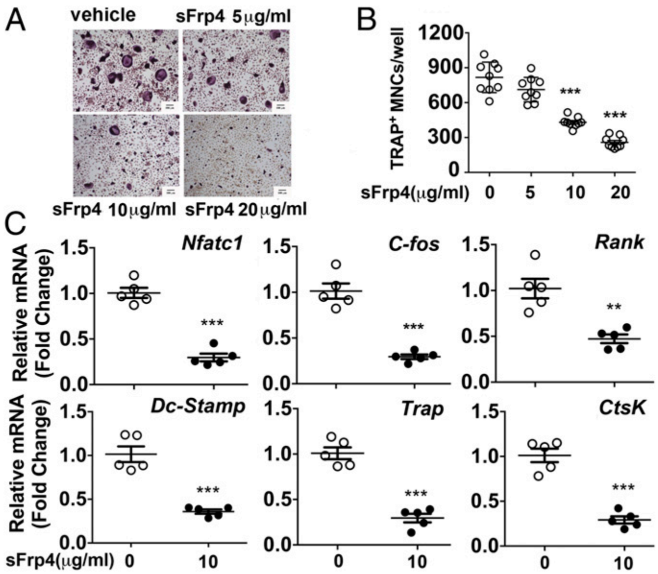

Fig. 2. sFrp4 treatment prevents early and late progenitor cells from developing into mature OCs. (*A* and *B*) TRAP staining (*A*) and quantification (*B*) in *wt* OCs treated w/wo increasing doses of sFrp4 ($n = 9$). (*C*) OC-specific gene expression in OCs treated w/wo sFrp4 (10 μg/mL) ($n = 5$). All data are mean ± SEM; open circles, vehicle; black circles, sFrp4-treated cells. $^{**}P < 0.005$, $^{***}P < 0.0001$. Student's *t* test vs. vehicle-treated cells. (Scale bars, 100 μm.)

Sfrp4 Mediates Osteoclastogenesis via the Noncanonical Wnt/Ror2/Jnk Cascade. As expected, *Sfrp4* deletion in OCs led to activation of both canonical Wnt/β-catenin and noncanonical Wnt/Jnk cascades (Fig. 4*A* and *SI Appendix*, Fig. S3*A*). Accordingly, sFrp4 treatment significantly suppressed both cascades in *wt* BMMs (*SI Appendix*, Fig. S3*B*). Given that canonical Wnt/β-catenin signaling suppresses OC differentiation while the noncanonical Wnt/Ror2/Jnk cascade promotes it (26, 28, 31), we hypothesized that Sfrp4 relies on the latter cascade to modulate OCgenesis. To test this hypothesis, we first blocked canonical Wnt/β-catenin signaling in $Sfrp4^{-/-}$ cells using increasing doses of the tankyrase inhibitor XAV939, which stimulates β-catenin degradation by stabilizing axin in the destruction complex (32) but not Jnk phosphorylation (Fig. 5*A*). As shown in Fig. 5 *B* and *C*, blocking canonical Wnt/β-catenin signaling had an additive effect on the increase in OC differentiation seen in $Sfrp4^{-/-}$ cultures. We then used $Cre\text{-}ER^{T2};Lrp5/6^{fl/fl}$ mice and generated $Lrp5/6^{fl/fl}$ deficient BMMs upon treatment with tamoxifen (Tam) in vitro (Fig. 5*D*). As shown in Fig. 5 *E* and *F*, knockout of Lrp5/6 coreceptors did not affect the ability of sFrp4 to suppress OCgenesis. In contrast, blocking the noncanonical Wnt/Ror2/Jnk cascade pharmacologically,

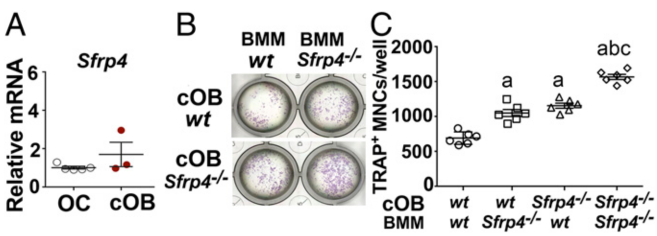

Fig. 3. Effects of BMM-secreted and OB-secreted Sfrp4 on OCgenesis. (*A*) *Sfrp4* gene expression in *wt* OCs and cOBs ($n = 3$ to 5). (*B* and *C*) TRAP staining (*B*) and quantification (*C*) in mixed-and-matched cocultures of BMMs and cOBs. All data are mean ± SEM. Two-way ANOVA followed by Tukey's test. $a < 0.0001$ vs. *cOBwt/BMMwt*, $b < 0.0001$ vs. *cOBwt/BMMSfrp4*$^{-/-}$, $c < 0.0001$ vs. *cOBSfrp4*$^{-/-}$*/BMMwt* ($n = 6$).

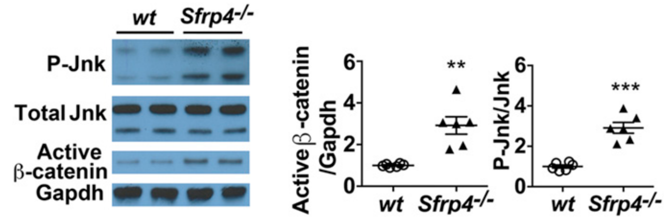

Fig. 4. Sfrp4 regulates both Wnt/β-catenin canonical and Wnt/Jnk noncanonical cascades in OCs. p-Jnk, total Jnk, and active β-catenin levels in *wt* and $Sfrp4^{-/-}$ BMMs. All data are mean ± SEM; open circles, *wt*; black triangles, $Sfrp4^{-/-}$ cells. $^{**}P < 0.005$, $^{***}P < 0.0001$. Student's *t* test vs. *wt* ($n = 5$ to 6).

via the selective Jnk inhibitor (Sp600125) (28) (Fig. 6*A*), significantly impaired the *Sfrp4* deficiency-dependent increased OCgenesis (Fig. 6 *B* and *C*). Confirming these data, knockout of the Ror2/Jnk axis, via in vitro excision of *Ror2* in $Cre\text{-}ER^{T2};Ror2^{fl/fl}$ BMMs, significantly reduced the ability of sFrp4 to block OCgenesis (Fig. 6 *D*–*F*). Moreover, sFrp4 significantly suppressed the Wnt5a-dependent induction of OCgenesis by blocking Wnt5a downstream activation of the Ror2/Jnk signaling cascade (Fig. 7) (28, 29). Excluding an overall change in Wnt ligand expression in the absence of *Sfrp4*, *Wnt5a* expression, as well as that of other key Wnts, was not changed in either $Sfrp4^{-/-}$ OC cultures or in cortical bone (*SI Appendix*, Fig. S4 *A* and *B*).

Recent studies have reported that Wnt3a can inhibit OC differentiation via a β-catenin–independent cAMP/PKA/pCreb pathway (31); we therefore assessed whether Sfrp4 might also utilize these alternative cascades. As shown in *SI Appendix*, Fig. S5, this pathway is not affected in $Sfrp4^{-/-}$ cultures. Likewise, the NF-κB/Tak1 and MAPK signaling pathways (that include ERK and P38 MAPKs), also involved in OCgenesis (31, 33–35), are unchanged in $Sfrp4^{-/-}$ cultures (*SI Appendix*, Fig. S5), therefore excluding a potential role for this signaling cascade downstream of Sfrp4 in BMMs. Similarly, and in contrast with OB-lineage cells (13), deletion of *Sfrp4* in OCs does not affect BMP signaling (*SI Appendix*, Fig. S4*C*). Altogether, these data demonstrate a key role for the Sfrp4/Ror2/Jnk axis in OCgenesis and support the hypothesis that in the absence of *Sfrp4*, noncanonical Wnt/Ror2/Jnk signaling activation in OCs overrides the negative effect of canonical Wnt/β-catenin signaling activation on OCgenesis.

***Ror2* Ablation in OCs In Vivo in *Sfrp4*$^{-/-}$ Mice Prevents the Increase in Endosteal Resorption and Partially Rescues Cortical Bone Mass.** These results prompted us to analyze whether Ror2 signaling is required for the action of Wnts on OCs in the absence of *Sfrp4* in vivo. For this purpose, we used male mice since *Sfrp4* deletion results in the same phenotype in males and females in both humans and mice (13, 21). We deleted *Ror2* in OCs using the *CtskCre* mice ($Ror2_{OC}$), and crossed them with $Sfrp4^{+/-}$ mice to obtain $Ror2^{fl/f}Sfrp4^{+/+}$, $Ror2_{OC}Sfrp4^{+/+}$, $Ror2^{fl/fl}Sfrp4^{-/-}$, and $Ror2_{OC}Sfrp4^{-/-}$ mice. $Ror2_{OC}$ mice develop high trabecular bone mass as a consequence of a significant decrease in OC number and function (28) but the cortical phenotype of these mice has not been described. Microcomputed tomography (μCT) analysis of the cortical midshaft demonstrated that, at 5 wk of age, deletion of *Ror2* in OCs does not significantly affect cortical bone. However, blocking the Ror2/Jnk axis in OCs in growing $Sfrp4^{-/-}$ mice significantly rescued the thinning of their cortical bone as well as their cortical area, although these parameters remain lower than in control and in $Ror2_{OC}$ mice (Fig. 8 *A* and *B* and *SI Appendix*, Table S1). In contrast, the marrow area and the total bone area were not rescued in $Ror2_{OC}Sfrp4^{-/-}$ mice (*SI Appendix*, Table S1). Bone histomorphometry analysis of the cortical midshaft revealed that deletion of *Ror2* in OCs in $Sfrp4^{-/-}$ mice prevents the increase in endosteal OC number and surface and significantly increases cortical thickness and cortical bone volume, although they remain significantly lower than in

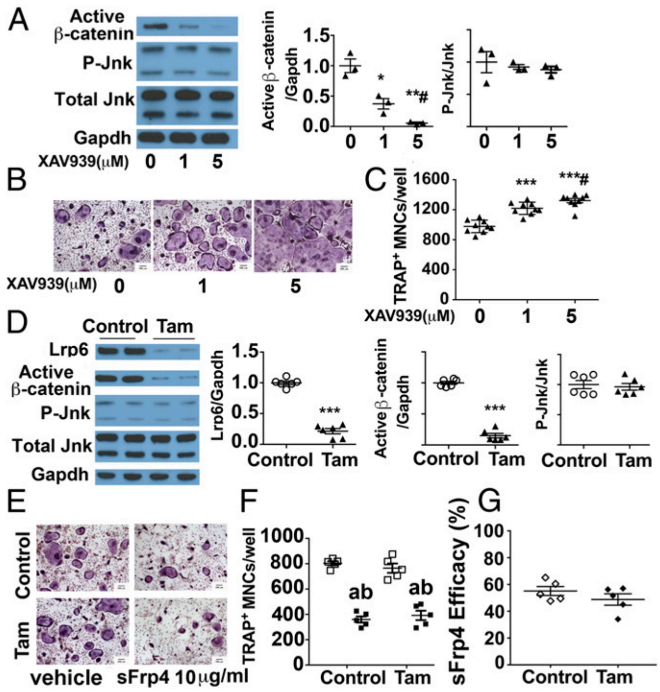

Fig. 5. Sfrp4 regulation of OCgenesis is independent of canonical Wnt/β-catenin signaling. (*A*) Active β-catenin, p-Jnk, and total Jnk levels in *Sfrp4*$^{-/-}$ OCs in the presence or absence of XAV939. Data are mean ± SEM; *$P < 0.05$, **$P < 0.005$ vs. untreated cells, $^{\#}P < 0.05$ vs. 1 μM XAV939. Student's *t* test ($n = 3$). (*B* and *C*) TRAP staining (*B*) and quantification (*C*) in *Sfrp4*$^{-/-}$ OCs treated w/wo XAV939. All data are mean ± SEM; ***$P < 0.001$ vs. untreated cells, $^{\#}P < 0.05$ vs. 1 μM XAV939. Student's *t* test ($n = 9$). (*D*) Lrp6, active β-catenin, p-Jnk, and total Jnk levels in Tam-treated and untreated (control) *Cre-ER*^{T2}*;Lrp5/6*$^{fl/fl}$ BMMs. Data are mean ± SEM; ***$P <$ 0.001 vs. control. Student's *t* test ($n = 6$). (*E* and *F*) TRAP staining (*E*) and quantification (*F*) in Tam-treated and control *Cre-ER*^{T2}*;Lrp5/6*$^{fl/fl}$ OCs in the presence of 10 μg/mL sFrp4 (black squares) or vehicle (open squares) ($n = 5$). All data are expressed as mean ± SEM; *a* < 0.0001 vs. control+vehicle, *b* < 0.0001 vs. Tam-treated+vehicle. Two-way ANOVA followed by Tukey's test ($n = 5$). (*G*) Sfrp4 efficacy in regulating TRAP⁺ MNCs in *Cre-ER*^{T2}*;Lrp5/6*$^{fl/fl}$ OCs. Data are mean ± SEM ($n = 5$). (Scale bars, 100 μm.)

Ror2$^{fl/f}$*Sfrp4*$^{+/+}$ mice (Fig. 8 *C* and *D*, Table 1, and *SI Appendix*, Fig. S6*A*). No significant difference in these parameters was seen in *Ror2*$_{OC}$*Sfrp4*$^{+/+}$ mice; however, a decrease in both the OC number and surface was observed (Fig. 8*D*, Table 1, and *SI Appendix*, Fig. S6*A*). The increase in marrow area was not rescued by *Ror2* OC-specific deletion in *Sfrp4*$^{-/-}$ mice and, as expected since the Ror2/Jnk cascade is deleted only in OCs, the decreased endosteal mineral apposition rate formation and bone formation rate were not rescued in *Ror2*$_{OC}$*Sfrp4*$^{-/-}$ mice (Table 1), explaining the only partial rescue of cortical thickness. μCT analysis of trabecular bone confirmed that at 5 wk of age, deletion of *Ror2* in OCs leads to increased trabecular bone volume and number as well as connectivity and decreased trabecular spacing and structure model index (SMI) (*SI Appendix*, Fig. S6*B* and Table S2). Consistent with our previous findings (13), *Ror2*$^{fl/fl}$*Sfrp4*$^{-/-}$ mice display increased trabecular bone mass and *Ror2* OC-specific deletion in *Sfrp4*$^{-/-}$ mice has an additive effect on trabecular bone volume, connectivity, and SMI compared with *Ror2*$^{fl/f}$*Sfrp4*$^{+/+}$ mice (*SI Appendix*, Fig. S6*B* and Table S2). These findings therefore support our hypothesis that Sfrp4 secreted in cortical bone by OB-lineage cells and/or by OCs themselves suppresses endosteal OCgenesis, at least in part, by blocking the noncanonical Wnt/Ror2/Jnk signaling cascade in OCs, an effect that in turn regulates cortical bone homeostasis.

Discussion

Our previous studies have shown that in the *Sfrp4* Pyle's disease mouse model, activation of the noncanonical Wnt/Jnk signaling cascade leads to decreased periosteal bone formation and deregulation of endosteal bone remodeling, all highly coordinated processes that define cortical thickness and homeostasis (13). Despite the clinical significance of the periosteum and the endosteum in determining cortical size, thickness, and strength, our basic understanding of their cellular characteristics and local or paracrine regulatory factors remains incomplete. *Sfrp4* is expressed in both trabecular and cortical bone. On the endosteal surface of cortical bone, *Sfrp4* is expressed by bone-lining cells and OBs (10, 11, 13, 22), suggesting that locally expressed and secreted Sfrp4 regulates OB and OC activity. We found here that, aside from being expressed by cells of the OB lineage (11, 13), *Sfrp4* is also expressed by OCs. Importantly, while we previously demonstrated that OB-expressed Sfrp4 regulates OCgenesis by regulating the Rankl/Opg ratio (13), the current studies suggest that Sfrp4-regulated signaling affects the OC lineage in an autocrine manner, broadening our understanding of this secreted protein beyond its role as a Wnt signaling inhibitor in the OB lineage (Fig. 8*E*). It has been shown that OB-secreted *Sfrp1* also impairs OCgenesis by binding to Rankl (36). A cell-autonomous effect of Sfrp1 in OCs has, however, not been reported. We found that if *Sfrp1* and *Sfrp2* expression is increased in *Sfrp4*$^{-/-}$ OCs, this is not enough to counteract the Wnt signaling activation seen in the absence of *Sfrp4*. In addition, the findings that *Sfrp1* deletion in mice results in a modest increase in trabecular bone mass and does not affect cortical bone thickness, or

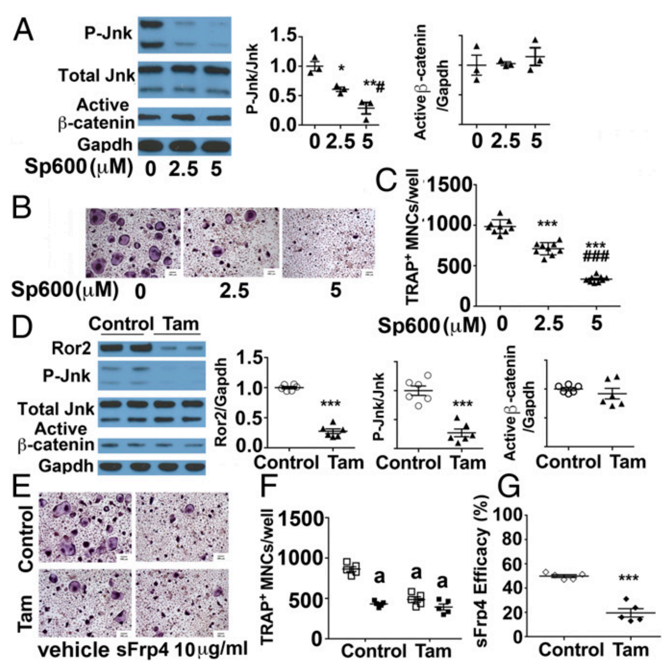

Fig. 6. Sfrp4 regulates osteoclastogenesis via the noncanonical Wnt/Ror2/Jnk cascade. (*A*) p-Jnk, total Jnk, and active β-catenin levels in *Sfrp4*$^{-/-}$ OCs w/wo SP600. Values are expressed as mean ± SEM; *$P < 0.05$, **$P < 0.005$ vs. untreated cells, $^{\#}P < 0.05$ vs. 2.5 μM SP600. Student's *t* test ($n = 3$). (*B* and *C*) TRAP staining (*B*) and quantification (*C*) in *Sfrp4*$^{-/-}$ OCs treated w/wo SP600 ($n = 9$). Data are mean ± SEM; ***$P < 0.001$ vs. untreated cells, $^{\#\#\#}P < 0.05$ vs. 2.5 μM SP600. Student's *t* test. (*D*) Ror2, p-Jnk, total Jnk, and active β-catenin levels in Tam-treated and untreated (control) *Cre-ER*^{T2}*;Ror2*$^{fl/fl}$ BMMs ($n = 5$ to 6). Data are mean ± SEM; ***$P < 0.001$ vs. control cells. Student's *t* test. (*E* and *F*) TRAP staining (*E*) and quantification (*F*) in Tam-treated and control *Cre-ER*^{T2}*;Ror2*$^{fl/fl}$ OCs in the presence of 10 μg/mL sFrp4 (black squares) or vehicle (open squares) ($n = 5$). Data are mean ± SEM; *a* < 0.0001 vs. control+vehicle. Two-way ANOVA followed by Tukey's test. (*G*) Sfrp4 efficacy in regulating TRAP⁺ MNCs in *Cre-ER*^{T2}*;Ror2*$^{fl/fl}$ OCs. Data are mean ± SEM; ***$P < 0.001$ vs. control cells. (Scale bars, 100 μm.)

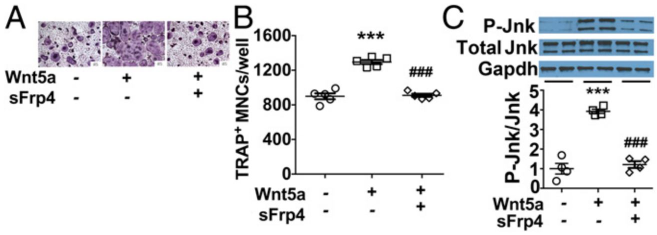

Fig. 7. Sfrp4 suppresses Wnt5-dependent induction of OCgenesis via the noncanonical Wnt/Ror2/Jnk cascade. (*A* and *B*) TRAP staining (*A*) and quantification (*B*) in *wt* Rankl-induced OCs treated w/wo Wnt5a (100 ng/mL) or sFrp4 (10 μg/mL) ($n = 5$). Data are mean ± SEM; $^{***}P < 0.01$ vs. untreated cells, $^{\#\#\#}P < 0.001$ vs. Wnt5a-treated cells. Student's *t* test. (*C*) p-Jnk and total Jnk levels in *wt* BMMs w/wo Wnt5a or sFrp4 ($n = 4$). (Scale bars, 100 μm.)

periosteal and endosteal circumference (37), establish that these secreted proteins have unique functions in regulating the cells involved in cortical homeostasis. Beyond their role as Wnt inhibitors, Sfrps were initially termed secreted apoptosis-related proteins based on the findings that they regulate cell viability in several cells and tissues including bone (38–41). Our studies, however, exclude a proapoptotic effect of Sfrp4 in OCs.

While there is strong evidence supporting a role for OB-dependent canonical Wnt signaling in the regulation of bone formation and bone resorption, the exact mechanisms by which this pathway affects bone mass via a cell-autonomous effect in OCs remain puzzling. Thus, in OCs, it has been shown that while canonical Wnt β-catenin cascade activation suppresses OCgenesis, noncanonical Wnt/Ror2/Jnk signaling activation favors it (23, 26–29). Because Sfrp4 acts as a Wnt ligand decoy receptor, its function in skeletal homeostasis is related to regulation of distinct Wnt signaling pathways. Our findings that the absence of Sfrp4 does not alter the expression of Wnt ligands suggest that most likely it is the local expression of specific Wnt ligands, frizzled receptors, and coreceptors they engage with that affects which downstream signaling cascades become active. Indeed, we have previously reported that while *Sfrp4* null calvarial OBs display activation of both the canonical Wnt/β-catenin and noncanonical Wnt/Jnk cascades, the canonical Wnt/β-catenin cascade is the only signaling activated in *Sfrp4* null bone marrow-derived OBs (13). In addition, the outcome of *Sfrp4* deletion in vivo is bone compartment-dictated: While *Sfrp4* deficiency unleashes the anabolic effect of canonical Wnt/β-catenin signaling activation in trabecular bone, which in turn leads to increased trabecular bone mass due to increased bone formation and no effect on OC number and bone resorption, activation of noncanonical Wnt/Jnk signaling in cortical bone impairs cortical bone mass by decreased periosteal and endosteal bone formation and increased endosteal resorption (13). Using both genetic and pharmacological approaches, we show that Sfrp4 impairs OC differentiation and activity, at least in part, via the regulation of the noncanonical Wnt/Ror2/Jnk cascade in OCs. Our in vivo findings that targeted deletion of *Ror2* in OCs rescues the number and surface of endosteal OCs in $Sfrp4^{-/-}$ mice demonstrate that the increase in endosteal resorption in $Sfrp4^{-/-}$ mice is a consequence of noncanonical Wnt/Ror2/Jnk signaling activation in OCs overriding the negative effect that activation of canonical Wnt/β-catenin signaling (also occurring in the $Sfrp4^{-/-}$ mice) has on OCgenesis (Fig. 8*E*). Interestingly, at 5 wk of age, while *Ror2* deletion in OCs increases trabecular bone mass, it does not significantly affect cortical thickness, although there is a decrease in the number and surface of endosteal OCs. This could be due to the age of the mice we analyzed and a cortical phenotype might develop over time in adult mice. Alternatively, it is plausible that Ror2 signaling in OCs is not sufficiently active under steady state, that is, in the presence of Sfrp4, to induce a cortical bone phenotype when deleted. In contrast, activation of Ror2 signaling in OCs in the absence of *Sfrp4* clearly favors endosteal OC differentiation and activity, suggesting that, when activated (in $Sfrp4^{-/-}$ mice and Pyle's disease), Ror2 signaling is critical in the induction of endosteal resorption. Thus, the finding that Sfrp4, secreted by both OBs and OCs, regulates OCgenesis via the noncanonical Wnt/Ror2/Jnk cascade might explain why in the trabecular bone of $Sfrp4^{-/-}$ mice, where this cascade in not activated (13), bone resorption is not affected. Although our studies demonstrate that Sfrp4 functions via the noncanonical Wnt/Ror2/Jnk cascade to regulate OCgenesis, one caveat of our studies is that in this model *Sfrp4* is globally deleted from all cells, osteoblasts, osteocytes, and osteoclasts included, and therefore not necessarily indicative of the specific and prominent role of osteoblast-, osteocyte-, or osteoclast-secreted Sfrp4 in vivo. Specific targeted deletion of *Sfrp4* in these cells will provide important mechanistic insights into the direct effect of OB-, osteocyte-, and OC-secreted Sfrp4.

Collectively, our studies show that OB- and OC-expressed *Sfrp4* regulates the differentiation and bone resorption activity of OCs via noncanonical Wnt/Ror2/Jnk signaling in OCs. Cortical expansion, thickness, and porosity are critical determinants of bone strength in several species including humans (42–44). Alterations in bone diameter, as in the deficient expansion seen with *Wnt16* or *Sfrp4* deletion, for instance, in thickness, as in Pyle's disease, or in osteoporosis all affect bone strength and lead to fragility fractures (1, 13, 45–51). Since endosteal bone remodeling is a determinant of cortical thickness and, even more clinically relevant, of cortical porosity, identifying the mechanisms by which Sfrp4 regulates cortical bone remodeling may help design novel therapeutic approaches for the treatment of diseases associated with bone fragility, bone healing, and bone regeneration.

Materials and Methods

Animals. *Sfrp4* null mice were previously described (13). *CtsKCre* mice were kindly provided by S. Kato, University of Tokyo, Tokyo, Japan, and $Lrp5/6^{fl/fl}$ mice were kindly provided by B. Williams, Van Andel Research Institute, Grand Rapids, MI. All animal studies are described in *SI Appendix*.

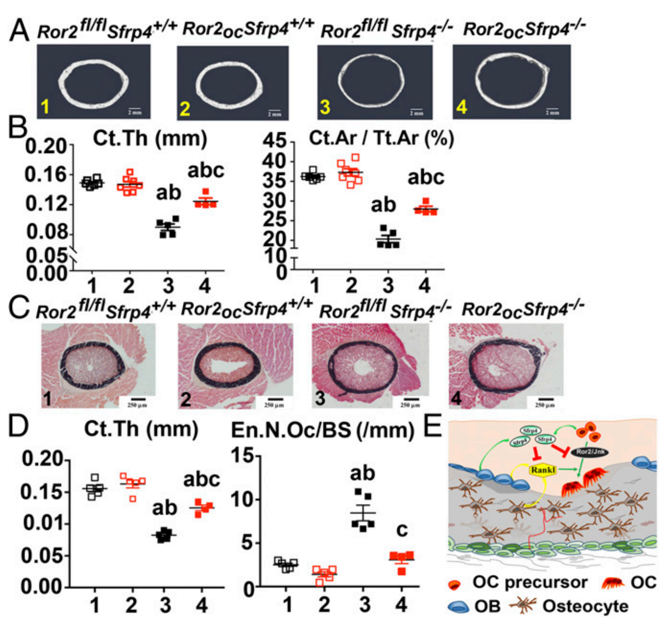

Fig. 8. OC-specific deletion of *Ror2* in $Sfrp4^{-/-}$ mice protects their cortical bone from excessive endosteal resorption. Skeletal phenotype of cortical bone of 5-wk-old male mice. (*A*) Representative μCT images. (Scale bars, 2 μm.) (*B*) Quantification of cortical bone parameters by μCT. Ct.Ar/Tt.Ar, bone area fraction; Ct.Th, cortical thickness. (*C*) Representative Von Kossa staining images. (Scale bars, 250 μm.) (*D*) Histomorphometric analysis. Ct.Th, cortical thickness; En.N.Oc/BS, endosteal osteoclst number/bone surface. All data are mean ± SEM ($n = 4$ to 7); $^{a}P < 0.005$ compared with $Ror2^{fl/fl};Sfrp4^{+/+}$ mice, $^{b}P < 0.005$ compared with $Ror2_{OC};Sfrp4^{+/+}$ mice, $^{c}P < 0.005$ compared with $Ror2^{fl/fl};Sfrp4^{-/-}$ mice. Two-way ANOVA followed by Tukey's test. (*E*) Working model. See text.

Cell Culture. Bone marrow macrophages were isolated from 6- to 8-wk-old *wt* and *Sfrp4*$^{-/-}$ mice as previously described (46). OC generation, treatment, and mixed-and-matched experiments are detailed in *SI Appendix*.

Tartrate-Resistant Acid Phosphatase Staining. TRAP staining was performed according to the manufacturer's protocol (Sigma-Aldrich). The number of TRAP^{+} cells with 2 or more nuclei per well was counted. BMMs from 5 to 9 distinct mice per genotype were used.

Bone Resorption Pit Assay. BMMs isolated from *wt* and *Sfrp4*$^{-/-}$ mice were treated with 30 ng/mL M-CSF and 10 ng/mL Rankl (both from R&D Systems) for 4 d to induce OCgenesis. Pit assay was performed as detailed in *SI Appendix*.

TUNEL Assay. *Wt* BMMs were cultured with 30 ng/mL M-CSF and 10 ng/mL Rankl w/wo sFrp4 (5 to 20 μg/mL) (R&D Systems) for 4 d. TUNEL assay was performed using an In Situ Cell Death Detection Kit, TMR red (Roche; 12156792910) according to the manufacturer's protocols.

Canonical Wnt/β-Catenin and Noncanonical Wnt/Ror2/Jnk Signaling Cascade Inhibition. For pharmacological inhibition and in vitro excision, BMMs were isolated from 6- to 8-wk-old mice and treated as detailed in *SI Appendix*.

Real-Time PCR. Total RNA was isolated from cells and cortical and trabecular bone and gene expression was determined as detailed in *SI Appendix*.

Western Analysis. Total proteins (10 μg) were resolved by SDS/PAGE under reducing conditions. Antibodies used and methods are detailed in *SI Appendix*.

Skeletal Phenotype. For microcomputed tomography scanning, a high-resolution desktop microtomographic imaging system (μCT35; Scanco Medical) was used to assess cortical and trabecular bone morphology as detailed in *SI Appendix*. Quantitative bone histomorphometric measurements were performed using the OsteoMeasure System as detailed in *SI Appendix*.

Statistical Analysis. Data are expressed as the mean ± SEM. Statistical analysis was conducted using unpaired two-tailed Student's *t* test. For comparison of three or more groups, two-way ANOVA followed by Tukey's multiple comparisons test for all groups was used. GraphPad PRISM 7 was used for statistical analysis. $P < 0.05$ was considered statistically significant.

ACKNOWLEDGMENTS. This work was supported by NIH–National Institute of Arthritis and Musculoskeletal and Skin Diseases Grant R01AR064724 (to R.B.) and by the China Scholarship Council (File 201606160044, to K.C.).

1. R. Baron, M. Kneissel, WNT signaling in bone homeostasis and disease: From human mutations to treatments. *Nat. Med.* **19**, 179–192 (2013).
2. Z. F. Zimmerman, R. T. Moon, A. J. Chien, Targeting Wnt pathways in disease. *Cold Spring Harb. Perspect. Biol.* **4**, a008086 (2012).
3. Y. Kawano, R. Kypta, Secreted antagonists of the Wnt signalling pathway. *J. Cell Sci.* **116**, 2627–2634 (2003).
4. C. M. Cruciat, C. Niehrs, Secreted and transmembrane Wnt inhibitors and activators. *Cold Spring Harb. Perspect. Biol.* **5**, a015081 (2013).
5. P. Bovolenta, P. Esteve, J. M. Ruiz, E. Cisneros, J. Lopez-Rios, Beyond Wnt inhibition: New functions of secreted frizzled-related proteins in development and disease. *J. Cell Sci.* **121**, 737–746 (2008).
6. Y. S. Cho *et al*., A large-scale genome-wide association study of Asian populations uncovers genetic factors influencing eight quantitative traits. *Nat. Genet.* **41**, 527–534 (2009).
7. D. Karasik, L. A. Cupples, M. T. Hannan, D. P. Kiel, Age, gender, and body mass effects on quantitative trait loci for bone mineral density: The Framingham Study. *Bone* **33**, 308–316 (2003).
8. D. Y. Lee *et al*., Association between polymorphisms in Wnt signaling pathway genes and bone mineral density in postmenopausal Korean women. *Menopause* **17**, 1064–1070 (2010).
9. U. Styrkarsdottir *et al*., Multiple genetic loci for bone mineral density and fractures. *N. Engl. J. Med.* **358**, 2355–2365 (2008).
10. R. Haraguchi *et al*., sFRP4-dependent Wnt signal modulation is critical for bone remodeling during postnatal development and age-related bone loss. *Sci. Rep.* **6**, 25198 (2016).
11. R. Nakanishi *et al*., Osteoblast-targeted expression of Sfrp4 in mice results in low bone mass. *J. Bone Miner. Res.* **23**, 271–277 (2008).
12. R. Nakanishi *et al*., Secreted frizzled-related protein 4 is a negative regulator of peak BMD in SAMP6 mice. *J. Bone Miner. Res.* **21**, 1713–1721 (2006).
13. P. O. S. Kiper *et al*., Cortical-bone fragility—Insights from sFRP4 deficiency in Pyle's disease. *N. Engl. J. Med.* **374**, 2553–2562 (2016).
14. E. Pyle, A case of unusual bone development. *J. Bone Joint Surg. Am.* **13**, 874–876 (1931).
15. R. J. Gorlin, M. F. Koszalka, J. Spranger, Pyle's disease (familial metaphyseal dysplasia). A presentation of two cases and argument for its separation from craniometaphyseal dysplasia. *J. Bone Joint Surg. Am.* **52**, 347–354 (1970).
16. N. Gupta, M. Kabra, C. J. Das, A. K. Gupta, Pyle metaphyseal dysplasia. *Indian Pediatr.* **45**, 323–325 (2008).
17. P. Beighton, Pyle disease (metaphyseal dysplasia). *J. Med. Genet.* **24**, 321–324 (1987).
18. M. Cohn, Konstitutionelle Hyperspongiosierung des Skeletts mit partiellem Riesenwuchs. *Fortschr Röntgenstr* **47**, 293–298 (1933).
19. N. G. Heselson, M. S. Raad, H. Hamersma, B. J. Cremin, P. Beighton, The radiological manifestations of metaphyseal dysplasia (Pyle disease). *Br. J. Radiol.* **52**, 431–440 (1979).
20. V. S. Narayananan, L. Ashok, G. P. Mamatha, A. Rajeshwari, S. S. Prasad, Pyle's disease: An incidental finding in a routine dental patient. *Dentomaxillofac. Radiol.* **35**, 50–54 (2006).
21. R. Brommage *et al*., High-throughput screening of mouse gene knockouts identifies established and novel skeletal phenotypes. *Bone Res.* **2**, 14034 (2014).
22. I. Matic *et al*., Quiescent bone lining cells are a major source of osteoblasts during adulthood. *Stem Cells* **34**, 2930–2942 (2016).
23. P. Ruiz *et al*., CathepsinKCre mediated deletion of βcatenin results in dramatic loss of bone mass by targeting both osteoclasts and osteoblastic cells. *Sci. Rep.* **6**, 36201 (2016).
24. R. Modarresi, Z. Xiang, M. Yin, J. Laurence, WNT/beta-catenin signaling is involved in regulation of osteoclast differentiation by human immunodeficiency virus protease inhibitor ritonavir: Relationship to human immunodeficiency virus-linked bone mineral loss. *Am. J. Pathol.* **174**, 123–135 (2009).
25. Y. W. Qiang *et al*., Characterization of Wnt/beta-catenin signalling in osteoclasts in multiple myeloma. *Br. J. Haematol.* **148**, 726–738 (2010).
26. W. Wei *et al*., Biphasic and dosage-dependent regulation of osteoclastogenesis by β-catenin. *Mol. Cell. Biol.* **31**, 4706–4719 (2011).
27. X. Sui *et al*., Constitutive activation of β-catenin in differentiated osteoclasts induces bone loss in mice. *Cell. Physiol. Biochem.* **48**, 2091–2102 (2018).
28. K. Maeda *et al*., Wnt5a-Ror2 signaling between osteoblast-lineage cells and osteoclast precursors enhances osteoclastogenesis. *Nat. Med.* **18**, 405–412 (2012).
29. S. Uehara *et al*., Protein kinase N3 promotes bone resorption by osteoclasts in response to Wnt5a-Ror2 signaling. *Sci. Signal.* **10**, eaan0023 (2017).
30. S. Angers, R. T. Moon, Proximal events in Wnt signal transduction. *Nat. Rev. Mol. Cell Biol.* **10**, 468–477 (2009).
31. M. M. Weivoda *et al*., Wnt signaling inhibits osteoclast differentiation by activating canonical and noncanonical cAMP/PKA pathways. *J. Bone Miner. Res.* **31**, 65–75 (2016).
32. S. M. Huang *et al*., Tankyrase inhibition stabilizes axin and antagonizes Wnt signalling. *Nature* **461**, 614–620 (2009).
33. S. E. Lee *et al*., The phosphatidylinositol 3-kinase, p38, and extracellular signal-regulated kinase pathways are involved in osteoclast differentiation. *Bone* **30**, 71–77 (2002).
34. X. Li *et al*., p38 MAPK-mediated signals are required for inducing osteoclast differentiation but not for osteoclast function. *Endocrinology* **143**, 3105–3113 (2002).
35. J. Mizukami *et al*., Receptor activator of NF-kappaB ligand (RANKL) activates TAK1 mitogen-activated protein kinase kinase kinase through a signaling complex containing RANK, TAB2, and TRAF6. *Mol. Cell. Biol.* **22**, 992–1000 (2002).
36. K. D. Häusler *et al*., Secreted frizzled-related protein-1 inhibits RANKL-dependent osteoclast formation. *J. Bone Miner. Res.* **19**, 1873–1881 (2004).
37. P. V. Bodine *et al*., The Wnt antagonist secreted frizzled-related protein-1 is a negative regulator of trabecular bone formation in adult mice. *Mol. Endocrinol.* **18**, 1222–1237 (2004).
38. H. S. Melkonyan *et al*., SARPs: A family of secreted apoptosis-related proteins. *Proc. Natl. Acad. Sci. U.S.A.* **94**, 13636–13641 (1997).
39. M. P. Alfaro *et al*., sFRP2 suppression of bone morphogenic protein (BMP) and Wnt signaling mediates mesenchymal stem cell (MSC) self-renewal promoting engraftment and myocardial repair. *J. Biol. Chem.* **285**, 35645–35653 (2010).
40. P. V. Bodine *et al*., The Wnt antagonist secreted frizzled-related protein-1 controls osteoblast and osteocyte apoptosis. *J. Cell. Biochem.* **96**, 1212–1230 (2005).
41. S. Pohl, R. Scott, F. Arfuso, V. Perumal, A. Dharmarajan, Secreted frizzled-related protein 4 and its implications in cancer and apoptosis. *Tumour Biol.* **36**, 143–152 (2015).
42. M. R. Allen, J. M. Hock, D. B. Burr, Periosteum: Biology, regulation, and response to osteoporosis therapies. *Bone* **35**, 1003–1012 (2004).
43. E. Seeman, Periosteal bone formation—A neglected determinant of bone strength. *N. Engl. J. Med.* **349**, 320–323 (2003).
44. R. M. Zebaze *et al*., Intracortical remodelling and porosity in the distal radius and post-mortem femurs of women: A cross-sectional study. *Lancet* **375**, 1729–1736 (2010).
45. R. Baron, E. Hesse, Update on bone anabolics in osteoporosis treatment: Rationale, current status, and perspectives. *J. Clin. Endocrinol. Metab.* **97**, 311–325 (2012).
46. S. Movérare-Skrtic *et al*., Osteoblast-derived WNT16 represses osteoclastogenesis and prevents cortical bone fragility fractures. *Nat. Med.* **20**, 1279–1288 (2014).
47. F. Gori, U. Lerner, C. Ohlsson, R. Baron, A new WNT on the bone: WNT16, cortical bone thickness, porosity and fractures. *Bonekey Rep.* **4**, 669 (2015).
48. K. L. Bell *et al*., Regional differences in cortical porosity in the fractured femoral neck. *Bone* **24**, 57–64 (1999).
49. V. Bousson *et al*., Distribution of intracortical porosity in human midfemoral cortex by age and gender. *J. Bone Miner. Res.* **16**, 1308–1317 (2001).
50. A. M. Parfitt *et al*., Bone histomorphometry: Standardization of nomenclature, symbols, and units. Report of the ASBMR Histomorphometry Nomenclature Committee. *J. Bone Miner. Res.* **2**, 595–610 (1987).
51. E. Seeman, Age- and menopause-related bone loss compromise cortical and trabecular microstructure. *J. Gerontol. A Biol. Sci. Med. Sci.* **68**, 1218–1225 (2013).